1. Ahmed Nasser B. Alsammak, 2. Ammar Shamil Ghanim

University of Mosul- College of Engineering- Electrical Engineering Dept. (1)(2)
ORCID: 1. 0000-0002-1248-4538, 2. 0000-0002-3602-5491

doi:10.15199/48.2023.10.33

Performance Enhancement and Assessment of the Dual Stator Induction Motor

Abstract: An induction motor with three phases is a sturdy and heavy-duty machine requiring little upkeep effort. However, it is associated with issues like load and driver type, speed regulation, and starting conditions. A variable frequency drive (VFD) can be used to drive the motor to address these issues; however, power electronics use is limited due to the high current needed for the motor. Multiple-phase motors address the high current problem using the three phases to supply the current required by the drives to run high-powered motors. Further, such motors are incredibly reliable and are less prone to faults. This paper evaluates the Dual-Stator Winding Induction Motor (DSIM) through simulation created using MATLAB to understand the motor operation and performance characteristics in steady and dynamic conditions. Simulation outcomes indicate that different operating characteristics are associated with enhanced motor efficacy.

*Streszczenie: Silnik indukcyjny z trzema fazami jest wytrzymałą i wytrzymałą maszyną, wymagającą niewielkich nakładów na konserwację. Wiąże się to jednak z takimi kwestiami, jak rodzaj obciążenia i kierowcy, regulacja prędkości i warunki rozruchu. Przemiennik częstotliwości (VFD) może być używany do napędzania silnika w celu rozwiązania tych problemów; jednak użycie energoelektroniki jest ograniczone ze względu na wysoki prąd potrzebny do silnika. Silniki wielofazowe rozwiązują problem wysokiego prądu, wykorzystując trzy fazy do dostarczania prądu wymaganego przez napędy do pracy silników o dużej mocy. Co więcej, takie silniki są niewiarygodnie niezawodne i mniej podatne na awarie. W niniejszym artykule dokonano oceny symulacji silnika indukcyjnego z podwójnym uzwojeniem (DSIM) stworzonej przy użyciu programu MATLAB, aby zrozumieć działanie silnika i charakterystykę wydajności w warunkach stabilnych i dynamicznych. Wyniki symulacji wskazują, że różne cechy operacyjne są związane ze zwiększoną sprawnością motoryczną. (**Poprawa wydajności i ocena silnika indukcyjnego z podwójnym stojanem**)*

Keywords: Dual Stator Induction Motor, DSIM, Multi-Phase Induction Motors, Matlab-Simulink.
Słowa kluczowe: Silnik indukcyjny z podwójnym stojanem, silniki indukcyjne wielofazowe, Matlab-Simulink.

Introduction

AC induction motors with drives are substituting DC motors. The former is versatile, cost-effective, reliable, and requires little maintenance. The AC motor faces a significant challenge concerning starting up and speed regulation; however, advances in power electronics and control mechanisms have reduced such challenges [1].

Drives addressed speed regulation for three-phase AC motors; however, these systems were infeasible for higher power levels because semiconductors have power limitations. Hence, drives can be coupled with multi-phase induction motors to address this challenge. Three-phase systems divide power and help reduce motor current and power regulation needs. Moreover, multi-phase motors offer better efficiency, improved torque density, higher fault tolerance, and fewer torque pulses [2-4]. Hence, high-power multi-phase drive and motor systems are used for ship propulsion, locomotives, and electric vehicles.

In DSIM systems, there are two possible approaches; with equal and unequal pole pairs, and with each approach, the displacement of the stator windings may be 0, 30, or 60 degrees. Based on equal pole pairs and different angle displacements between stator windings, DSIM performance is examined and analyzed in this study.

Literature Review and Problem Statement

There was a time when the literature had few references concerning multi-phase induction motors. Such works about multi-phase induction motors indicate that their benefits over typical three-phase systems have been anticipated [2]. The asymmetrical six-phase design of the induction motor is a fascinating consideration for high-power requirements. The dual stator may exist with equal pole pairs or unequal pole pairs for each winding set, and for equal pole pair, the two sets of stators are displaced either by 30 degrees which are called asymmetrical windings or 0, 60 degrees, called symmetrical winding[4-6].

A dual stator induction motor (DSIM) comprises two individual stator windings in a three-phase configuration having a shared machine core; it has a typical squirrel cage rotor winding. A symmetrical system comprises winding sets placed at 60^{o}, while asymmetrical systems comprise 30^{o} angles to enhance performance. This approach was proposed by Ward and Harer [7] in 1969. The researchers demonstrated and assessed an inverter-driven five-phase induction motor. They recommended that torque pulsation could be decreased using a higher stator phase count. Nelson and Krause [8] used computers to simulate three different designs of inverter-fed six-phase motors. They indicated that using 30° phase belts could remove the torque pulsation at the sixth harmonic, typically characteristic of inverter-based three-phase motors. Nevertheless, there was a rise in peak stator current levels.

G.K. Singh [9] 2003 devised a straight forward d-q approach for a multi-phase induction system, which is suitable for assessing the motor's dynamic, transient, and steady-state characteristics when running under balanced loads. This analytical framework considered the system's behaviour under mutual leakage reactance concerning both three-phase windings. This framework was devised considering a general reference and can be used to assess machine operation at any displacement angle.

The previous decade witnessed rapid advancements in power electronics, smart control systems, and electronic process systems. There has been renewed interest in DSIM to limit industrial challenges about starting and running high loads with better reliability and lower harmonics issues [10].

The probable advantages concerning a multi-phase induction motor are due to the six-phase system having a 30° displacement angle for the two coil systems that nullify air gap flux harmonics having an order of ($6n\pm1$, n=1, 3, 5…). Hence, losses pertaining to the copper rotor on these and torque harmonics having an order of (6n, n=1, 3, 5…) are nullified if a voltage source inverter (VSI) drives the system. The major benefit is that the system can start and function even when a single stator phase is under a short circuit or open. Moreover, the phase-specific current is lower without higher phase voltage, lesser harmonics

concerning the DC link, and higher power and reliability are other advantages [1].

Since induction motors with dual stators are typically regulated using AC drives [11] or transformer driven by a three-phase supply [12], their dynamic characteristics must be assessed comprehensively to extract higher performance from the setup. This paper employs the MATLAB-Simulink model to evaluate the dual stator induction motor (DSIM) and assess its performance under severe perturbations with a deep, comprehensive approach.

Three-phase induction motors' performance typically suffers because of the adverse impact of pulsating torque on the voltage across the inverter drive [13] and [14]. A DSIM with proper winding characteristics and a VSI system can help increase performance substantially [15]. This study used 0, 30°, and 60° separation across the stator windings on a DSIM system. An assessment highlights the impact of connection on torque properties, system response, and current waveform. The significance of modelling lies in its capability to generate a broad range of analyses for transient and steady-state responses under various operating conditions without the associated drawbacks of overheating or excessive mechanical stress that may occur during actual testing [16].

Dual Stator Induction Motor (DSIM) Model

The DSIM comprises one squirrel cage rotor and dual three-phase stator windings, as depicted in Figure (1) [17] .

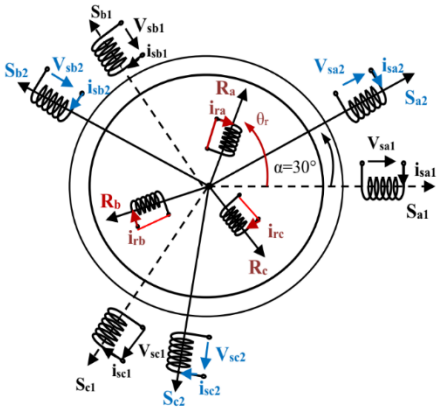

Fig.1. Dual stator induction machine schematic.

Modelling DSIMs can help improve design and control algorithms, enhancing machine performance, reliability, and efficiency. This can lead to a reduction in costs and an increase in knowledge and understanding of these complex systems. In addition to these benefits, modelling DSIMs can also help identify potential issues and provide insights into how to address them. This ensures that these machines operate at optimal levels.

Six-Phase Induction Machine: Assessment and Simulation

Electric drives suffer due to stator voltage changes, leading to pulsating torque. It is best to have the least feasible pulsating torque. It is feasible to control pulsating torque for rectifier-inverter-based drives. Several inverters can be combined with the appropriate number of three-phase windings set across adequate displacements on the system. Such an arrangement is feasible using an induction system with dual three-phase stator windings and one rotor winding. A 30° displacement schematic for stator windings is depicted in Figure (1).

System performance can be specified directly using the expressions in the following section. Figure (2) depicts an equivalent Circuit in the two-axis plane. Further, primed quantities are applied to the stator using the desired turn ratio. Interestingly, there is a transformation concerning windings' relative position, as determined through applicable voltage (V_{qsl}, V_{qs2}, V_{dsl}, V_{ds2}) in Figure (2), rather than using variables concerning the three-axis equivalent circuit. Figure (1) depicts a system with several three-wire connections, allowing the elimination of zero quantities [6].

Double stator induction machine d-q equivalent circuit

Several assumptions were made while formulating the set of expressions that model an induction motor having several three-phase windings. These are:

1. Uniform air gap
2. Negligible winding and friction loss, saturation, and eddy currents
3. Sinusoidal winding arrangement across the air gap
4. Identical windings in a set
5. Winding sets are not connected

Figure (2) depicts the d-q equivalent circuit using an arbitrary DSIM reference frame [9].

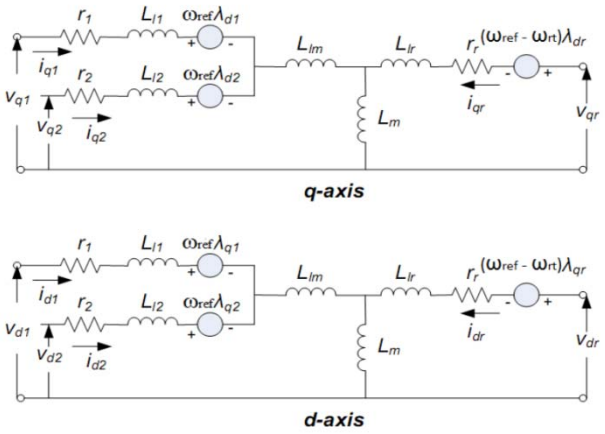

Fig.2. The dq-axis equivalent circuit for dual stator induction machine [18]

The following expressions specify the voltage vectors for six-phase stator and three-phase rotor coils [9]:

$$\overrightarrow{v_s} = r_s \overrightarrow{i_s} + \rho \overrightarrow{\lambda_s} + j\omega_k \overrightarrow{\lambda_s} \quad (1)$$

$$\overrightarrow{v'_r} = r'_r \overrightarrow{i'_r} + \rho \overrightarrow{\lambda'_r} + j(\omega_k - \omega_r)\overrightarrow{\lambda'_r} \quad (2)$$

Where ω_k depicts angular velocity using the coordinate system, hence, the machine's voltage expressions for an arbitrary reference frame are:

$$v_{sq1} = r_{s1} i_{sq1} + \omega_k \lambda_{d1} + \rho \lambda_{q1} \quad (3)$$

$$v_{sd1} = r_{s1} i_{sd1} - \omega_k \lambda_{q1} + \rho \lambda_{d1} \quad (4)$$

$$v_{sq2} = r_{s2} i_{sq2} + \omega_k \lambda_{d2} + \rho \lambda_{q2} \quad (5)$$

$$v_{sd2} = r_{s2} i_{sd2} - \omega_k \lambda_{q2} + \rho \lambda_{d2} \quad (6)$$

$$v'_{rq} = r'_r i'_{rq} - (\omega_k - \omega_r)\lambda'_{rd} + \rho \lambda'_{rq} \quad (7)$$

$$v'_{rd} = r'_r i'_{rd} - (\omega_k - \omega_r)\lambda'_{rq} + \rho \lambda'_{rd} \quad (8)$$

The equations from (9) to (14); express the flux induced in each winding in both the stator and rotor

$$\lambda_{q1} = L_{l1} i_{q1} + L_{lm}(i_{q1} + i_{q2}) + L_m(i_{q1} + i_{q2} + i_{qr}) - L_{ldq} i_{d2} \quad (9)$$

(10) $\lambda_{q2} = L_{l2} i_{q2} + L_{lm}(i_{q1} + i_{q2}) + L_m(i_{q1} + i_{q2} + i_{qr}) + L_{ldq} i_{d1}$

(11)

$$\lambda_{d1} = L_{l1} i_{d1} + L_{lm}(i_{d1} + i_{d2}) + L_m(i_{d1} + i_{d2} + i_{dr}) + L_{ldq} i_{q2}$$

(12) $\lambda_{d2} = L_{l2} i_{d2} + L_{lm}(i_{d1} + i_{d2}) + L_m(i_{d1} + i_{d2} + i_{dr}) - L_{ldq} i_{q1}$

(13) $\lambda_{qr} = L_{lr} i_{qr} + L_m(i_{q1} + i_{q2} + i_{qr})$

(14) $\lambda_{dr} = L_{lr} i_{dr} + L_m(i_{d1} + i_{d2} + i_{dr})$

Now, by using the state space approach and considering the equations mentioned above, with currents as the state variable and flux linkage as the dependent variable, the following state space equation can be written based on stator and rotor currents:

(15) $\left[V\right] = \left[R\right]\left[I\right] + \left[L\right]\left[I^{\bullet}\right]$

Where:

the input vector: $\left[V\right] = \left[V_{q1}, V_{q2}, V_{d1}, V_{d2}, V_{qr}, V_{dr}\right]$

And the state vector $\left[I^{\bullet}\right] = \left[\rho I_{q1}, \rho I_{q2}, \rho I_{d1}, \rho I_{d2}, \rho I_{qr}, \rho I_{dr}\right]$

The current matrix: $\left[I\right] = \left[I_{q1}, I_{q2}, I_{d1}, I_{d2}, I_{qr}, I_{dr}\right]$

and the coeffivient martrices [R], [L] are :

$$[R] = \begin{bmatrix} R_1 & 0 & W_{l1} & W(L_2 + L_{dq}) & 0 & WL_m \\ -WL_{dq} & R_2 & WL_2 & WL_1 & 0 & WL_m \\ -WL_1 & -WL_2 & R_1 & WL_{dq} & -WL_m & 0 \\ -WL_2 & -WL_1 & -WL_{dq} & R_2 & -WL_m & 0 \\ 0 & 0 & -W_{sl}L_m & -W_{sl}L_m & R_r & -W_{sl}L_3 \\ -W_{sl}L_m & -W_{sl}L_m & 0 & 0 & -W_{sl}L_3 & Rr \end{bmatrix}$$

$$[L] = \begin{bmatrix} L_1 & L_2 & 0 & -L_{dq} & L_m & 0 \\ L_2 & L_1 & L_{dq} & 0 & L_m & 0 \\ 0 & L_{dq} & L_1 & L_2 & 0 & L_m \\ -L_{dq} & 0 & L_2 & L_1 & 0 & L_m \\ L_m & L_m & 0 & 0 & L_3 & 0 \\ 0 & 0 & L_m & L_m & 0 & L_3 \end{bmatrix}$$

where $L_1 = L_{ls} + L_{lm} + L_m, L_2 = L_{lm} + L_m$
$and\ \ L_3 = L_{lr} + L_m,\ W_{sl} = W_k - W_r$

Using the equations mentioned above: the model of Figure (3). Was permitted

Performance Enhancement by Loss Minimisation

It is critical to assess dual stator induction motor loss (P_{loss}) because the windings are small but complex. The analysis for the three-phase stator is shown in references [19] and [20]. This study neglects convertor, stray, windage, and friction losses. Using Figure (2), the total loss is expressed as:

$$p_{loss} = p_{cus1} + p_{cus2} + p_i + p_{cus1}$$

(16) $p_{loss} = r_{s1}(i_{sq1}^2 + i_{sd1}^2) + r_{s1}(i_{sq2}^2 + i_{sd2}^2) + r_f' i_{f2} + r_r'(i_{rq}^2 + i_{rd}^2)$

considering identical dual stator windings, $r_{s1} = r_{s2} = r_s$, and $i_{sq1} = i_{sq2} = i_{sq}$, $i_{sd1} = i_{sd2} = i_{sd}$, which is a special case for an identical position for the two stator winding sets, also the Iron losses ($r_f' i_{f2}$) are considered negligible because $r_f' \gg r_r'$. Hence Equation (16) is expressed as:

(17) $p_{loss} = 2r_s(i_{sq}^2 + i_{sd}^2) + r_r'(i_{rq}^2 + i_{rd}^2)$

Now, according to the mathematical deriving methodology mentioned in (19); the current passing throw the rotor resistance is due to quadratic axis stator current (i_{qs}) only, so equation (17) will be further simplified to:

(18) $p_{loss} = 2r_s i_{sd}^2 + (2r_s + r_r) i_{sq}^2$

The dynamic behavior for torque and speed are defined with equations(19),(20):

(19) $T_e = (3/2)(p/2)(1/\omega_b)\left[(i_{sq1} + i_{sq2})\varphi_{md} - (i_{sd1} + i_{sd2})\varphi_{mq}\right]$

(20) $(\omega_r/\omega_b) = (1/p)[(1/\omega_b)(p/2)(1/J)(T_e - T_l)]$

Iron losses are ignored, and torque can also be specified as:

(21) $T_e = (3/2)(p/2)(L_m)\left[(i_{sq1} + i_{sq2})(i_{sd1} + i_{sd2})\right]$

(22) $T_e = k_t(i_{sq})(i_{sd})$

So, from the last equation $i_{sq}(i_{sd}) = \frac{T_e}{K_t * i_{sd}}$

$$\frac{dp_{loss}}{di_{sd}} = 4r_s i_{sd} + 2(2r_s + r_r) i_{sq}(i_{sd}) \frac{di_{sq(isd)}}{di_{sd}}$$

(23) $\frac{dp_{loss}}{di_{ds}} = 4r_s i_{sd} - 2(2r_s + r_r)\frac{i_{sq}^2}{i_{sd}} = 0$

Equation (23) is used to derive the following expressions:

(24) $i_{sd}^2 = \frac{r_r + 2r_s}{2r_s} i_{sq}^2$

(25) $\frac{i_{sd}}{i_{sq}} = \sqrt{\frac{r_r + 2r_s}{2r_s}}$

The above analysis indicates that the losses can be made as low as possible when the relationship between the two components of the stator current is regulated, as in eq. (25); Therefore, the inclusion of this relationship in the control algorithms is used further to enhance and improve the action of the inverter as a voltage source supplies the machine model proposed in this work.

Proposed DSIM Model

MATLAB-Simulink was used to model the DSIM using matrix in Equation (15). System parameters are specified in Table (1), while the DSIM schematic is depicted in Figure (3).

Table (1) Dual Stator Induction Machine parameters [9].

parameter	Value
R_1	0.0847Ω
R_2	0.0847Ω
X_{l1}	0.0543Ω
X_{l2}	0.0543Ω
R_r	0.0376Ω
X_{lr}	0.0543Ω
X_m	1.521 Ω
X_{lm}	0.03 Ω
X_{ldq}	0.00 Ω
H	0.6 N.m

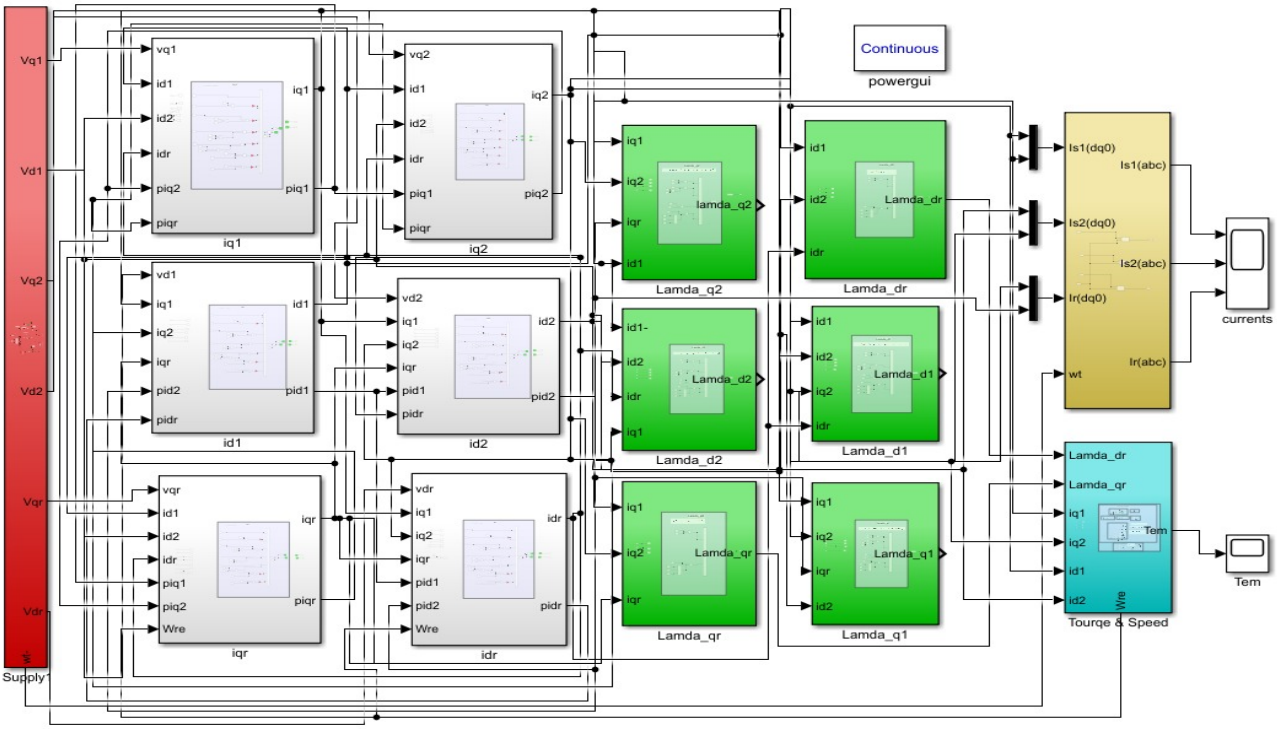

Fig.3. MATLAB-Simulink-based Dual stator induction machine model

Test Outcomes and Discussion

Figures (4-10) depict the DSIM outcomes concerning mutual flux association, torque, speed, rotor, and stator currents for 0, 30°and 60° balanced supply-fed system.
This study and several other research works concerning 30° displacement-based six-phase induction motors indicate better torque for this displacement. Flux time harmonics of order (6n+1; n =1, 3, 5, 7 …) concerning the air gaps are minuscule. Consequently, better sinusoidal characteristics are expected for rotor and dq-axis stator currents at 30°. All harmonic-associated copper losses at the rotor, including harmonic torque associated with orders (6n; n =1, 3, 5, 7 ...), are almost eliminated when a six-step VSI is employed. Therefore, 30° displacements are associated with minimum rotor heat generated due to harmonic losses. Moreover, the assessment indicates that this displacement is associated with higher stator currents, which are attributed to more stator current harmonics. Figures (4-11) depict operational outcomes for the proposed system driven using a six-step supply; these outcomes consider zero and non-zero stepped loadings. Figure (7) indicates the low overshoot in losses with 30° compared with 0°and 60°. Figure (8) explains how the divergence between the quadrature components of currents was increased with the increase of angle displacement of two stator winding.

A 30° displacement does not create rotor pulsations. Moreover, pulsation and torque average 5% in contrast to 20% and 30% for 0° and 60° displacements. Further, Figures (12)-(13) indicate system performance when driven using a PWM inverter voltage source. Speed changes, rotor current, and torque are more uniform for 30° displacement than 0° and 60° configurations. Nevertheless, the system does not provide noteworthy performance gains when driven using six-step voltages. One significant disadvantage concerning the square-wave three-phase drives is the substantial ripple that causes noise and inflicts mechanical stress on the rotor bearings and loads. Mitigation comprises full-pitch windings better equipped to handle voltage harmonics for motors with significant phases.

Figure (14) depicts the applied mechanical Load (Tmech). VSI-driven load for theta=30° is assessed in Figures (15) and (16), where response speed and torque are measured against time.

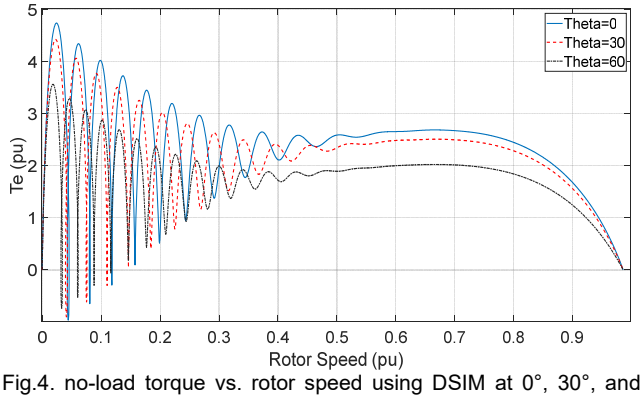

Fig.4. no-load torque vs. rotor speed using DSIM at 0°, 30°, and 60°displacements across the winding sets.

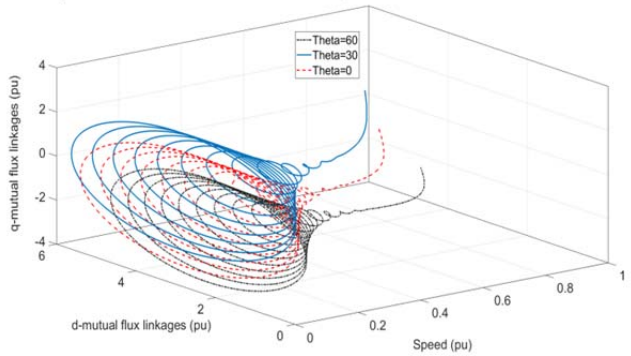

Fig.5. dq mutual flux linkages vs. rotor speed using DSIM at 0°,30°, and 60°displacements (theta) between the stator winding sets.

Stator and rotor current values are depicted against time using Figures (17-20). The system uses varied load (Tmech) across 30° and 60° theta values for a VSI-powered

system. It is evident that losses and currents differ. There is about 30% less current at 30°. Validation of the model was carried out by comparing the torque characteristics expressed in Figure (6) with those reported in [8], which are essentially the same, with the same machine rating.

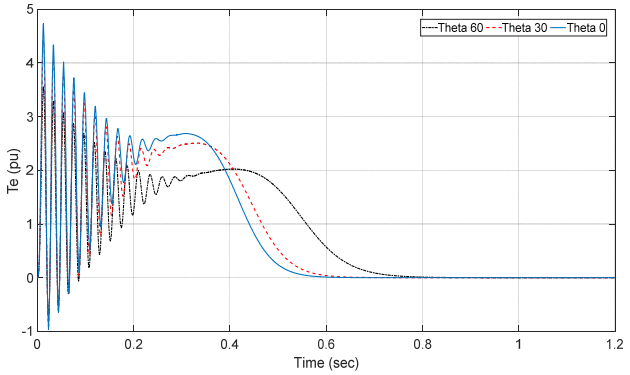

Fig.6. No-load DSIM torque vs. time for 0°,30°, and 60°displacements (theta) between the stator winding sets.

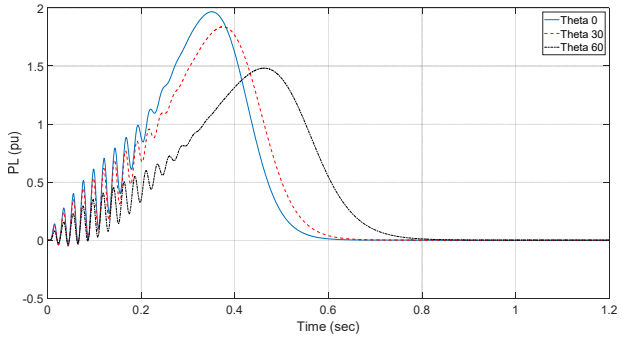

Fig.7. Power loss vs. time for 0°,30°, and 60°displacements (theta) between the stator winding sets.

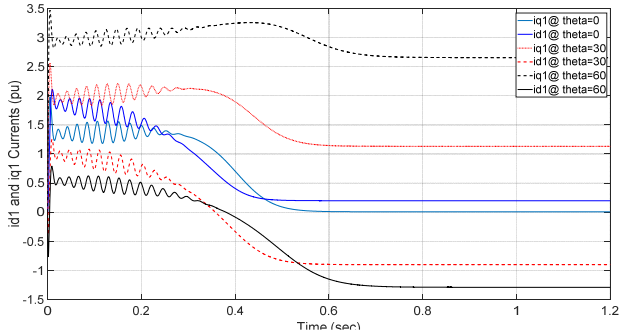

Fig.8. DSIM dq currents for first winding vs. time for 0°,30°, and 60° displacement (Theta) between the stator winding sets.

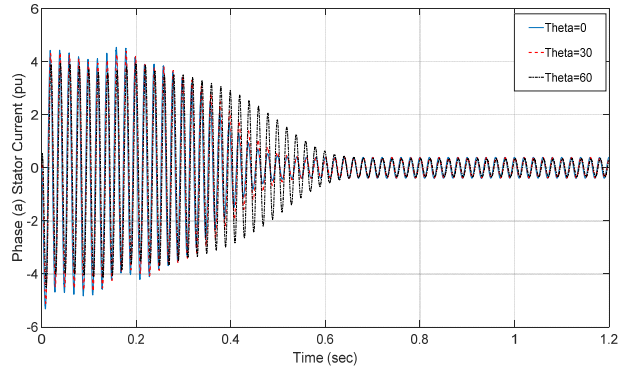

Fig.9. DSIM phase (a) for first winding vs. time for 0°,30°, and 60° displacement (Theta) between the stator winding sets.

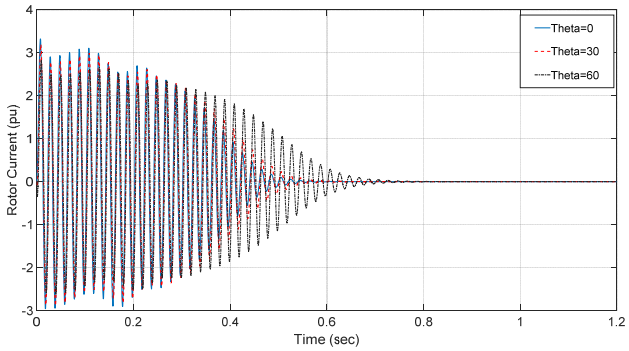

Fig.10. SIM rotor current vs. time for 0°,30°, and 60°displacements (theta) between the stator winding sets.

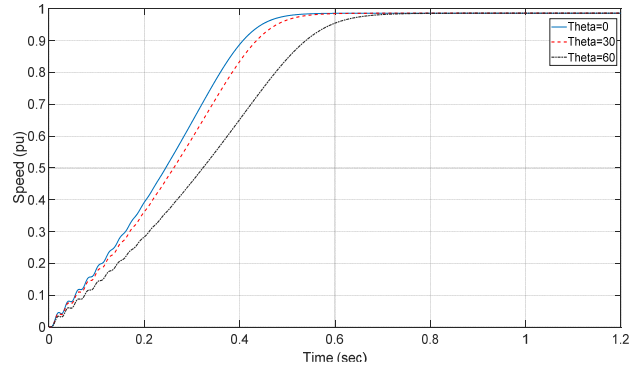

Fig.11. No-load torque vs. time for 0°,30°, and 60° displacements (theta) between the stator winding sets.

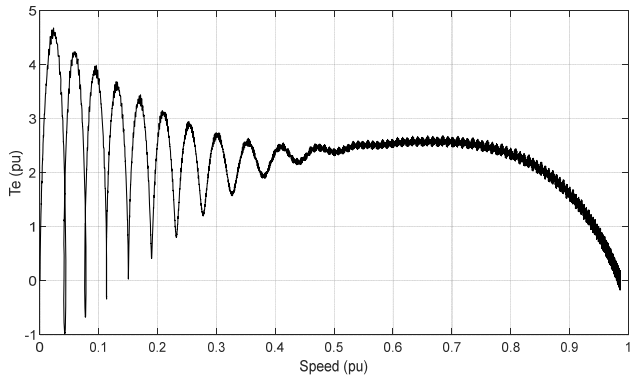

Fig.12. No-load torque vs. time for theta=30°, supplied using VSI.

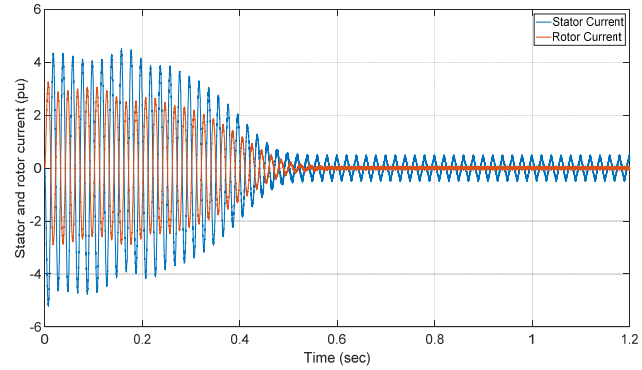

Fig.13. No-load stator and rotor currents vs. time for theta=30°, supplied using VSI.

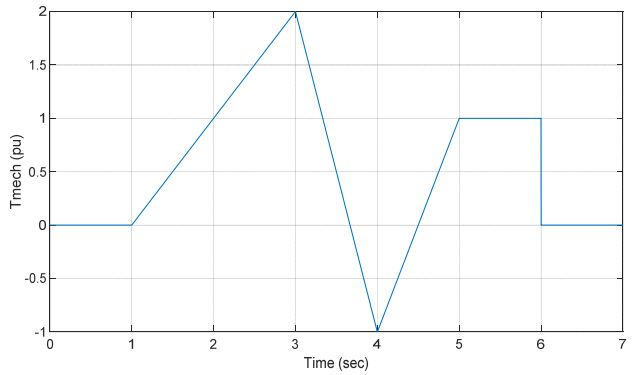

Fig.14. Applied Mechanical Load (Tmech) vs. time.

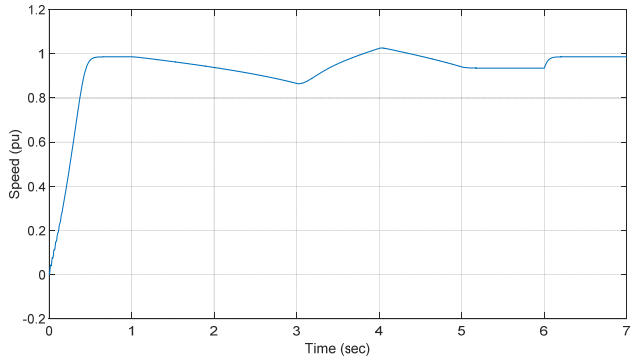

Fig.15. Speed vs. time with variation load (Tmech) for theta=30° and VSI-based supply.

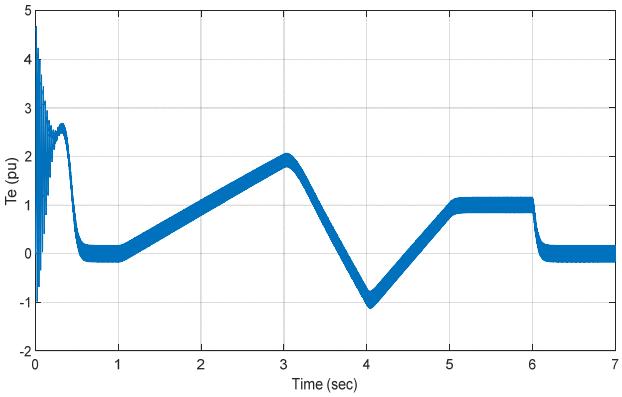

Fig.16. Torque vs. time with varying load (Tmech) for theta=30° and VSI-based supply.

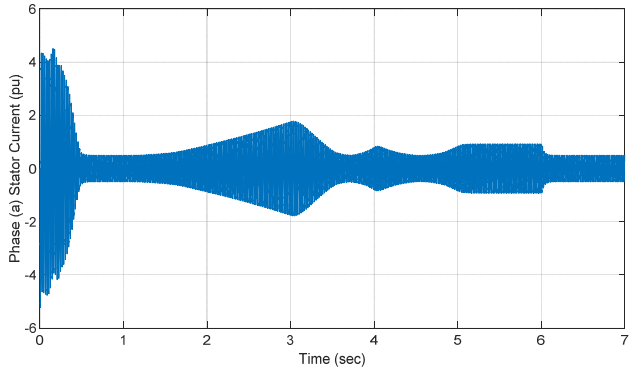

Fig.17. Phase(a) stator current vs. time with varying load (Tmech) for theta=30° and VSI-based supply

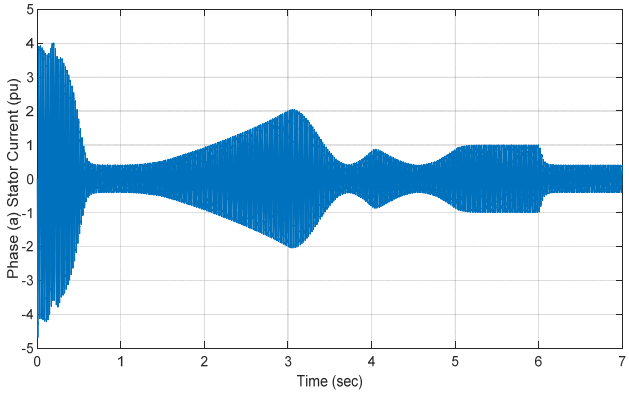

Fig.18. Phase (a) stator current vs. time with varying load (Tmech) for theta=60° and VSI-based supply

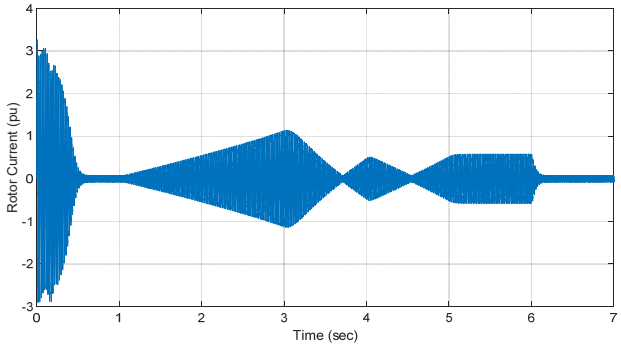

Fig.19. Rotor current vs. time with variation load (Tmech) for Theta=30° and VSI-based supply.

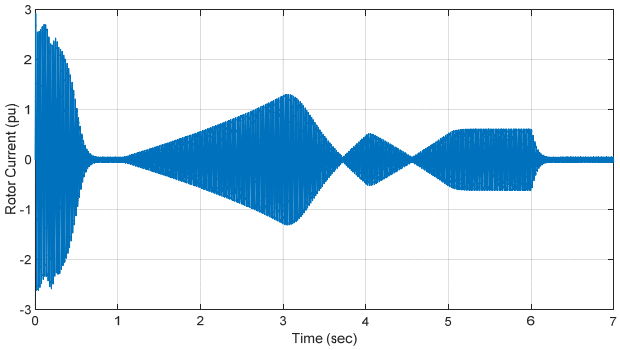

Fig.20. Rotor current vs. time with varying load (Tmech) for theta=60° and VSI-based supply.

Conclusions

In this paper, a revised, extended state-space model based on field and armature currents was developed and reported in the synchronous park transformation. A typical modelling and assessment technique is devised to assess the dual stator induction motor (DSIM) three-phase windings with and without symmetry. MATLAB-Simulink was used to model a six-phase induction motor powered using two six-step inverters. The inverters' action were enhanced by applying a loss minimization algorithm (LMA) to minimize losses at light load. This model helped assess and enhance machine torque properties. The DISM with the 0, 30°, and 60° displacements between stator winding are studied with the proposed model. An assessment indicated how connection configurations affect current waveforms, torque properties, and motor response. The configuration specified in this study offers substantial benefits because double inverters can drive machines directly without shared loads and transformers. The suggested mathematical framework can be used to formulate adjustable drives for induction motor control to obtain the required starting properties.

Nomenclature

T_L	Torque load
VSI	voltage source inverter
P	Pole count
j	moment of inertia
ω_{bs}	base speed
ω_{ks}	reference frame speed
ω_{rs}	rotor speed
ρ	differentiation
V_{sq1}, V_{sd1}	q- and d-axis voltages for stator winding set I
V_{sq2}, V_{sd2}	q- and d-axis voltages for stator winding set II
λ_{q1}, λ_{d1}	q- and d-axis stator flux linkages for set I
λ_{q2}, λ_{d2}	q- and d-axis stator flux linkages for set II
λ_{qr}, λ_{dr}	q- and d-axis rotor flux linkages corresponding to stator set I
i_{sq1}, i_{sd1}	q- and d-axis currents for stator winding set I
i_{sq2}, i_{sd2}	q- and d-axis currents for stator winding set II
r_{s1}	per phase stator resistance for the set I
r_{s2}	per phase stator resistance for the set II
r_r'	per phase rotor resistance concerning the stator
L'_{lm}	Shared mutual leakage inductance concerning the two stator windings
L_m	Stator-rotor mutual inductance
L_{l1}	per phase leakage inductance for stator winding set I
L_{l2}	per phase leakage inductance for stator winding set II
L'_{lr}	per phase leakage inductance for rotor winding referred to the stator
X'_{lm}	shared mutual leakage reactance between the two stator windings
X_m	stator-rotor mutual reactance
X_{l1}	per phase leakage reactance for stator winding set I
X_{l2}	per phase leakage reactance for stator winding set II
X'_{lr}	per phase leakage reactance for rotor winding referred to the stator
L'_{ldq}	mutual between the d- and q-axis stator winding circuit
v'_{rq},v'_{rd}	q- and d-axis rotor voltages referred to the stator

Acknowledgements

The authors thank the University of Mosul / College of Engineering for the provided facilities that helped to complete this work.

***Authors**: Assistant Prof. Dr. Ahmed Nasser B. Alsammak, University of Mosul - College of Engineering - Electrical Engineering Dept.* Postal Code *41002, E-mail: ahmed_alsammak@uomosul.edu.iq*
Assistant Lec. Mr. Ammar Shamil Ghanim, University of Mosul - College of Engineering - Electrical Engineering Dept. Postal *Code 41002, E-mail: ammarshamilhanon@uomosul.edu.iq*

REFERENCES

[1] Singh GK. Multi-phase induction machine drive research - A survey. Electr Power Syst Res. 2002;61(2):139–47.

[2] Parsa L. On advantages of multi-phase machines. In: 31st Annual Conference of IEEE Industrial Electronics Society, 2005 IECON 2005 [Internet]. IEEE; 2005. p. 6 pp. Available from: http://ieeexplore.ieee.org/document/1569139/

[3] Benyoussef E, Barkat S. Five-level Direct Torque Control with Balancing Strategy of Double Star Induction Machine. Int J Syst Appl Eng Dev. 2020;14(Dci):116–23.

[4] Ben Slimene M, Khlifi MA. Investigation on the Effects of Magnetic Saturation in Six-Phase Induction Machines with and without Cross Saturation of the Main Flux Path. Energies. 2022;15(24).

[5] Kokila A, Senthil Kumar V. Design and Analysis of Dual Output Three Level Inverter with Reduced Switch Count Topology. IETE J Res. 2020;

[6] Khoshhava MA, Zarchi HA, Markadeh GA. Optimal Design of a Dual Stator Winding Induction Motor with Minimum Rate Reduction Level. IEEE Trans Ind Electron. 2021;68(2):1016–24.

[7] Ward EE, Härer H. Preliminary investigation of an invertor-fed 5-phase induction motor. Proc Inst Electr Eng. 1969;116(6):980.

[8] Nelson RH, Krause PC. Induction machine analysis for arbitrary displacement between multiple winding sets. IEEE Trans Power Appar Syst. 1974;PAS-93(3):841–8.

[9] Singh GK, Pant V, Singh YP. Voltage source inverter driven multi-phase induction machine. Comput Electr Eng. 2003;29(8):813–34.

[10] Muñoz AR, Lipo TA. Dual Stator.Pdf. IEEE Trans Ind Appl. 2000;36(5):1369–79.

[11] Ziane D, Azib A, Taib N, Rekioua T. Study and design of the direct torque control of double star induction motor. J Electr Syst. 2013;9(1):114–24.

[12] Abdelwanis MI, Rashad EM, Taha IBM, Selim FF. Implementation and control of six-phase induction motor driven by a three-phase supply. Energies. 2021;14(22).

[13] Zagirnyak M, Kalinov A, Melnykov V. Sensorless vector-control system with the correction of stator windings asymmetry in induction motor. Prz Elektrotechniczny. 2013;89(12):340–3.

[14] C B. Minimization of Torque Ripple in Induction Motor Drive by Optimal Harmonic Elimination. Przegląd Elektrotechniczny. 2022;1(4):38–41.

[15] Abdel-Khalik AS, Abdel-Majeed MS, Ahmed S. Effect of Winding Configuration on Six-Phase Induction Machine Parameters and Performance. IEEE Access. 2020;8(December):223009–20.

[16] Ghanim AS, Alsammak ANB. Modelling and Simulation of Self-Excited Induction Generator Driven By a Wind Turbine. Eastern-European J Enterp Technol. 2020;6(8):6–16.

[17] Boukhalfa G, Belkacem S, Chikhi A, Benaggoune S. Direct torque control of dual star induction motor using a fuzzy-PSO hybrid approach. Appl Comput Informatics. 2018.

[18] Pal BK, Member S, Prajapati P, Member S, Bajaj M. Control of Grid Side Converter for Grid Connected Six Phase Induction Generator. 2019;(April).

[19] Uddin MN, Nam SW. New online loss-minimization-based control of an induction motor drive. IEEE Trans Power Electron. 2008;23(2):926–33.

[20] Hesari S, Hoseini A. A new approach to improve induction motor performance in light-load conditions. J Electr Eng Technol. 2017;12(3):1195–202.